Published in final edited form as:
Hear Res. 2007 October ; 232(1-2): 1–19. doi:10.1016/j.heares.2007.06.011.

Closure of supporting cell scar formations requires dynamic actin mechanisms

Andrew J. Hordichok and **Peter S. Steyger**
Oregon Hearing Research Center, Oregon Health & Science University, 3181 SW Sam Jackson Park Road, Portland, Oregon, 97239

Abstract

In many vertebrate inner ear sensory epithelia, dying sensory hair cells are extruded, and the apices of surrounding supporting cells converge to re-seal the epithelial barrier between the electrochemically-distinct endolymph and perilymph. These cellular mechanisms remain poorly understood. Dynamic microtubular mechanisms have been proposed for hair cell extrusion; while contractile actomyosin-based mechanisms are required for cellular extrusion and closure in epithelial monolayers. The hypothesis that cytoskeletal mechanisms are required for hair cell extrusion and supporting cell scar formation was tested using bullfrog saccules incubated with gentamicin (6 hours), and allowed to recover (18 hours). Explants were then fixed, labeled for actin and cytokeratins, and viewed with confocal microscopy. To block dynamic cytoskeletal processes, disruption agents for microtubules (colchicine, paclitaxel) myosin (Y-27632, ML-9) or actin (cytochalasin D, latrunculin A) were added during treatment and recovery.

Microtubule disruption agents had no effect on hair cell extrusion or supporting cell scar formation. Myosin disruption agents appeared to slow down scar formation but not hair cell extrusion. Actin disruption agents blocked scar formation, and largely prevented hair cell extrusion. These data suggest that actin-based cytoskeletal processes are required for hair cell extrusion and supporting cell scar formation in bullfrog saccules.

Keywords

Hair cell; extrusion; cell death; actin; myosin; microtubules; supporting cells; inner ear; saccule; vestibular system; in vitro

Introduction

Aminoglycoside antibiotics, like gentamicin, are ototoxic drugs that induce hearing loss and vestibular disorders (Miller, 1985), and nephrotoxicity (Humes, 1999). Aminoglycosides selectively kill sensory hair cells that are then extruded from amphibian inner ear sensory epithelia (Baird et al., 1996), chick basilar papillae (Cotanche et al., 1990; Duncan et al., 2001) and mammalian vestibular organs (Duvall et al., 1963; Lang et al., 1997; Li et al., 1995a). In the bullfrog saccule, each hair cell has a round apex and is surrounded by five to

Correspondence should be addressed to: P.S. Steyger, Ph.D., Oregon Hearing Research Center, Oregon Health & Science University, 3181 Sam Jackson Park Road, Portland, OR 97239 USA. FAX: (+1) 503-494-5656, Voice: (+1) 503-494-1062, E-mail: steygerp@ohsu.edu.

seven supporting cells that are characterized by their polygonal apical surfaces (Baird et al., 1996). When dying hair cells are extruded, the surrounding supporting cells expand their apical processes to seal the potential breach beneath the hair cell, and produce a supporting cell scar formation (Fig. 1), which is characterized by a multi-cellular actin ring (Steyger et al., 1997). This process is necessary to maintain the electro-chemical separation between endolymph and perilymph bathing the apical and baso-lateral membranes of cells at the surface of the scala media (Forge, 1985; Meiteles et al., 1994).

The actin cytoskeleton participates in a variety of cellular activities, including cell division, cell motility, induction of cell polarity, and membrane trafficking (Brown et al., 2001). Disruption of filamentous actin (F-actin) assembly interferes with the extrusion of dying epithelial cells in confluent epithelial cell cultures and subsequent epithelial closure (Rosenblatt et al., 2001). Inhibition of myosin function in these same cells also disrupts apoptotic cell extrusion. Therefore, we hypothesized that disruption of actin or myosin activity could interfere with the extrusion of dying hair cells and the closure of the supporting cell scar formations.

Li et al. (1995a) hypothesized that hair cell microtubules play an essential role during the extrusion process. Microtubule assembly is inhibited by colchicine binding at the polymerization end of the microtubule, resulting in the eventual depolymerization of the microtubular filament (Bergen et al., 1983; Platts et al., 1999). Dynamic microtubular processes can also be disrupted by taxol which stabilizes microtubules by preventing microtubule depolymerization and normal turnover of tubulin subunits (Arnal et al., 1995). Therefore, we also tested the hypothesis that disruption of dynamic microtubular activity could interfere with the extrusion of dying hair cells and the closure of the supporting cell scar formations. Here we report the effects of six cytoskeletal disruption agents (summarized in Fig. 2) on the extrusion of bullfrog saccular hair cells during cytotoxic insult *in vitro*. The data demonstrate that only actin disruption agents significantly prevent hair cell extrusion, and concomitantly arrest the expansion of the supporting cell apical processes, preventing supporting cell scar formation.

Materials and Methods

All reagents were from Sigma (Saint Louis, MO) unless otherwise stated.

Animals/Specimens

Healthy adult bullfrogs (*Rana catesbeiana*) were anesthetized in 0.2% MS-222. The temporal bones were dissected in ice-cold, oxygenated (95% O_2 and 5% CO_2) HEPES-buffered saline (HBS), containing 110 mM Na^+, 2 mM K^+, 4 mM Ca^{2+}, 120 mM Cl^-, 3 mM D-glucose, and 5 mM HEPES, pH 7.25 (Steyger et al., 1998; Steyger et al., 1997). The saccule was isolated and the otolithic membrane removed by proteolytic digestion in oxygenated 50 μg/ml subtilopeptidase BPN for 15 minutes. The digested remains of otolithic membrane were subsequently removed by gentle mechanical agitation.

Treatment

Freshly-excised saccular explants were incubated at 25°C for 24 hours in amphibian culture media (GIBCO, Carlsbad, CA) supplemented with 10% egg ultrafiltrate (Wolf et al., 1964). To induce hair cell death, saccular explants were treated with 200 μg/ml gentamicin in amphibian culture media (ACM) for six hours, washed three times with ACM and further incubated with ACM for 18 hours prior to fixation (Baird et al., 1996; Steyger et al., 1997). Some explants were also incubated in the presence of cytoskeletal disruption agents for 24 hours. To disrupt microtubule activity, 10 μM colchicine or 0.1 μM paclitaxel (taxol) (Kim et al., 2002; Platts et al., 1999) was used. Cytochalasin D (1 μM) and latrunculin A (5 μM) were

used to block dynamic actin activity. To inhibit myosin kinetics, 100 μM Y-27632 (VWR, West Chester, PA) and 50 μM ML-9 (Platts et al., 1999; Rosenblatt et al., 2001) were used. Control explants were also treated with these cytoskeletal disruption agents in the absence of gentamicin to determine if these cytoskeletal inhibitors alone induced hair cell extrusion. There were at least three explants for each group, with the left ear providing the control explant for the experimentally-treated explant from the contra-lateral (right) ear.

Fluorescence labeling

All explants were fixed in 4% formaldehyde in 0.1 M phosphate buffer, pH 7.25, for 1 hour. After rinsing in 0.02 M phosphate buffered saline (PBS), explants were permeabilized for 10 minutes with 0.5% Triton X-100 in PBS. Actiniferous structures were labeled for F-actin using phalloidin-conjugated AlexaFluor-568 (Molecular Probes, OR), diluted 1:50 in PBS for 1 hour. Some explants were immunolabeled for cytokeratins; after Triton X-100 permeabilization, nonspecific binding sites were blocked by immersion in 1% bovine serum albumin (BSA), 10% goat serum in PBS for 30 minutes, and then incubated with 1:100 mouse anti-cytokeratin antibodies (clone K8.13, immunoreactive for epithelial human cytokeratin polypeptides 10, 11 and 18; Sigma) in PBS with 1% BSA overnight at 4°C. After rinsing, the primary antibody was detected using AlexaFlour-488 anti-mouse IgG (Molecular Probes; 1:100) in 1% BSA in PBS for 1 hour at room temperature. Immunocytochemical controls were processed in the absence of primary antisera. After rinsing, explants were post-fixed for 30 minutes, rinsed, whole-mounted in Vectashield (Vector Laboratories, Burlingame, CA), coverslipped, and sealed with clear nail varnish.

Confocal Microscopy

Explants were imaged using an 8-bit Bio-Rad MRC 1024 ES laser scanning confocal system (Hercules, CA) attached to a Nikon Eclipse TE300 inverted microscope (Melville, NY). Confocal images were collected using a 60x objective lens (numerical aperture 1.4) in 1024 × 1024 pixel frames with an *xy* resolution = 240 nm and *xz* resolution = 400 nm, and post-processed using Bio-Rad LaserSharp imaging software, and Photoshop (Adobe).

Hair bundle density

Labeled organs were also imaged using 10x and 20x objectives to determine the macular area (Figure 2) and hair cell density. Overlapping images acquired with a 20x objective were used to form a composite image of the entire organ and a manual count of hair cells was performed. Hair cells were counted as present if they displayed a hair bundle and cuticular plate intact with the plane of the sensory epithelium.

Transmission light microscopy

Explants, treated with or without gentamicin and/or cytoskeletal inhibitors, were immersion-fixed with 3% glutaraldehyde and 1.5% formaldehyde in 0.1 M phosphate buffer, pH 7.2, overnight. Following dehydration through an ascending alcohol series, explants were infiltrated with glycol methacrylate (Polysciences, Warrington, PA), polymerized, cross-sectioned at 3 μm parallel to the saccular nerve, and stained with methylene blue and basic fuchsin (Pillers et al., 2002). Qualitative morphologic evaluations of the sectioned saccule were made with a 40x (air) objective on a Leica DMLB microscope to determine the presence or absence of hair cell extrusions and sensory epithelial integrity in regions of scar formations. Images were captured digitally using a Nikon Coolpix 4500.

Western blotting

For immunoblots, six adult otoconia-free vestibular labyrinths were homogenized in cell lysis buffer (0.15 M NaCl, 0.5% Triton X-100, 0.2% SDS in 0.05 M Tris) containing protease and

phosphorylation inhibitors (200 μM PMSF, 1 μM leupeptin, 1 μM pepstatin, 1 mM Na fluoride and 300 μM Na orthovanadate). Samples were analyzed for total protein content using Bio-Rad DC microplate protein assay. Proteins were separated on 10% SDS-PAGE gels for 2 hours at 100 volts and either stained with 1% Coomassie Blue or electrophoretically transferred onto nitrocellulose membranes for 2 hours at 60 volts. Transferred proteins were blocked with 10% dried milk, probed with cytokeratin antisera, then HRP-labeled secondary antibodies, visualized with chemiluminesence buffers and documented in the darkroom with OrthoMax Blue film.

Transmission electron microscopy

Saccular explants were fixed with 4% formaldehyde plus 2.5% glutaraldehyde in 0.1 M phosphate buffer for 2 hours, dehydrated through an ascending alcohol series, passaged through propylene oxide, and subsequently infiltrated with Epon-812 (Ted Pella, Redding, CA) over 48 hours, prior to resin polymerization at 60°C for 48 hours. Ultra-thin sections were obtained on an ultra-microtome (Leica Ultra-cut, Bannockburn, IL), collected on colloidin-coated slot grids, stained with 2% aqueous uranyl acetate, and lead citrate prior to observation with a Philips CM 100 transmission electron microscope (FEI, Hillsboro, OR).

Results

Hair bundle density

The left ear provided the control saccular explant (incubated with or without cytoskeletal inhibitors) and the right ear the experimental saccular explant (gentamicin-treated with or without cytoskeletal disruption agents). At time-point 0, there was a statistically negligible difference (1.8%) in the density of hair bundles between the right ear (87.8 +/− 2.2 bundles per 10,000 μm², n=3) and left ear (89.4 +/− 4.3 per 10,000 μm², n=3, $p > 0.05$). After 24 hours of incubation in ACM alone (left saccule), there was a statistically significant drop in hair bundle density (81.4 +/− 4.4; n=4) compared to time-point 0 ($p < 0.01$).

After incubation with 200 μg/ml gentamicin for six hours and subsequent recovery in ACM for 18 hours (right saccule), there was a further drop in hair bundle density (73.6 +/− 3.6; n=4) compared to the left saccule after 24 hours incubation in ACM alone (81.4 +/− 4.4; n=4). Thus, a six hour incubation with 200 μg/ml of gentamicin induced a statistically significant drop ($p < 0.05$) in hair bundle density (and presumably hair cell bodies) greater than in control explants 24 hours after explantation. Both experimental insults (explantation, and subsequent drug treatment) enabled us to test our hypothesis that cytoskeletal disruption agents modulate hair cell extrusion from the sensory epithelium and subsequent supporting cell scar formation *in vitro*.

Explants treated with colchicine (microtubule disruption agent) alone had a statistically significant drop ($p < 0.01$) in hair bundle density compared to control explants incubated with ACM only. Hair bundle densities in explants treated with taxol (microtubule disruption agent) or an actin disruption agent (latrunculin A or cytochalasin D) alone were not significantly different from control explants incubated with ACM only (see Table 2 for bundle densities; $p > 0.1$). Explants treated with ML-9 and Y-27632 (myosin disruption agents) alone also had a significant drop ($p < 0.05$) in hair bundle density compared to control explants incubated in ACM only (for Y-27632 conditions, n=2).

Incubation of explants with gentamicin alone significantly decreased hair bundle density compared to control contra-lateral explants incubated with ACM only ($p < 0.01$). When gentamicin was added to explants treated with any cytoskeletal disruption agent, there was always a statistically significantly drop in hair bundle density compared to contra-lateral

explants treated with disruption agents alone ($p < 0.05$). When explants treated with both cytoskeletal disruption agents and gentamicin were statistically compared to those treated with gentamicin alone, colchicine, ML-9 and Y-27632 induced a statistically significant drop in hair bundle density over and above that induced by gentamicin alone ($p < 0.01$; Table 2).

Phalloidin histochemistry of surface preparations

At low resolution, explants treated with gentamicin alone displayed greater loss of hair bundles (Figure 3B) than in explants incubated with ACM only (Figure 3A). At higher resolution, the location of missing hair bundles was characterized by multi-cellular fluorescent-labeled actin rings (Fig. 3C). These phalloidin-labeled rings represent the F-actin component of the junctional complex in each supporting cell with that of the now-departed hair cell. Within this ring, the newly-expanded apices of the supporting cells which meet near the center of the missing hair cell's former position, giving rise to the characteristic cartwheel-like appearance of supporting cell scar formations in bullfrog vestibular sensory organs (Baird et al., 1996).

Microtubule disruption agents

There was little difference in the distribution of phalloidin labeling in explants receiving microtubule disruption agents alone (Fig. 3D–I) compared to explants treated without disruption agents their absence (Fig. 3A–C). However, hair bundle loss was visibly greater in gentamicin-treated explants (Fig. 3E,H) compared to control explants treated with microtubule disruption agents alone (see Fig. 3D,G). High resolution imaging of scar formations revealed characteristic multi-cellular phalloidin rings in all explants treated with gentamicin (Fig. 3C,F,I, Fig. 4C–E).

In colchicine-treated explants, deposition of F-actin was also observed within the central region of each newly-expanded apical process of supporting cells participating in the scar formation (Fig 4A,D). No deposition of F-actin could be seen in the central region of expanded supporting cell apices of scar formations in gentamicin-treated explants (Fig. 4C), nor in taxol-treated explants (Fig. 4B,E). This was verified using the Thermo look-up table (LUT). Supporting cell apices not participating in scar formations are red or dark red in the center of supporting cell apices, regardless of treatment, demonstrating low or undetectable levels of F-actin deposition. However, in colchicine-treated explants (Fig. 4G) the expanded supporting cell apices showed higher (yellow) fluorescent intensity levels of F-actin compared to the lower (dark red) intensity levels of F-actin in expanded apices of supporting cells in scar formations of explants treated with gentamicin only (Fig. 4F) or gentamicin plus taxol (Fig. 4H). Nonetheless, microtubule disruption agents did not halt the morphogenesis of supporting cell scar formations.

Myosin disruption agents

Low resolution images of explants treated with myosin disruption agents Y-27632 or ML-9 revealed substantial hair bundle loss (Fig. 5A,E). Explants treated with these myosin disruption agents plus gentamicin (Fig. 5B,F) showed greater hair bundle loss compared to myosin disruption agent treatment only (Fig. 5, and Table 2). High resolution confocal imaging of explants treated with Y-27632 (Figs. 5C,D) or ML-9 (Fig. 5G,H) revealed a mix of completely closed scar formations, and partially-closed scar formations identified by an incomplete expansion of supporting cell apices within the phalloidin-labeled multicellular actin rings; particularly in ML-9 treated explants. Partially-closed scar formations were never seen in gentamicin-treated only explants in this experimental paradigm. Frequently, closed scars appeared weakly-labeled with fluorescent phalloidin and structurally disorganized (Fig. 5D,H) compared to those seen in gentamicin-treated only explants (as in Fig. 3C). Partially-closed scars also appeared to display negligible phalloidin labeling at the leading edges of newly-expanding supporting cell apical processes (Fig. 5H).

Actin disruption agents

In low resolution imaging, explants treated with gentamicin and actin disruption agents (Fig. 6B, F) contained greater numbers of missing hair bundles compared to explants treated with actin inhibitors only (Fig. 6A,E). These bundleless areas were distinguished by black circular areas in the epithelium not seen in other explants. Higher resolution imaging of areas containing missing hair bundles showed black circular or ovoid areas in the sensory epithelium, that were more clearly-defined in latrunculin A-treated explants (Fig. 6G) than in cytochalasin D-treated explants (Fig. 6C). These areas did not contain supporting cell scar formations that were identified in explants not treated with actin disruption agents. In cytochalasin D-treated explants, higher intensity F-actin phalloidin labeling occurs at the junctional confluence between two adjacent supporting cells, and the location of the "missing" hair cell (Fig. 6D). In latrunculin A-treated explants (Fig. 6H), and other non-cytochalasin D-treated explants (data not shown), no sub-apical accumulation of intense fluorescence was observed at the confluence of supporting cells surrounding "missing" hair cells, as seen in cytochalasin D-treated explants.

Hair cell extrusions: transmission light microscopy

After incubation in ACM alone for 24 hours, few cellular extrusions are seen above the sensory epithelium in sections of explants treated in the absence of gentamicin or cytoskeletal inhibitors (Fig. 7A). Sections from explants fixed 18 hours after a 6 hour incubation with gentamicin revealed cellular extrusions above the sensory epithelium (Fig. 7B). All explants co-incubated with colchicine, taxol (microtubule disruption agents), ML-9 or Y-27632 (myosin disruption agents) had extrusions above the sensory epithelium (Fig. 7C–F, respectively). However, explants treated with actin disruption agents (cytochalasin D and latrunculin A) did not display any cellular extrusions, and had translucent hair cell bodies embedded within the sensory epithelium (Figs 7G,H, respectively). Additionally, in explants treated with cytochalasin D, fine protrusions of cellular material extend from the apices of supporting cells into the extracellular fluid (Fig. 7G).

Hair cell extrusions: cytokeratin immunolabeling

Preliminary studies revealed that hair cell extrusions could be identified immunocytochemically in wholemounts of saccular epithelia using cytokeratin antibodies (Fig. 1). Explants incubated with secondary antibodies alone revealed negligible fluorescence (data not shown). This antibody is cross-reactive with three distinct protein bands, 43, 45 and 56/56.5 (Fig. 8A lower inset), that correspond to keratin polypeptides: pp 19, pp 18, and pp 10 and pp 11 (as a single band) respectively (Moll et al., 1982). When bullfrog saccules were fixed immediately after peptidase treatment to remove the otolithic membrane, distinctive cytokeratin labeling is localized in supporting cell apices, outlining the round apices of hair cells (Fig. 8A). However, at higher resolution, cytokeratin labeling is preferentially localized in the polygonal apices of supporting cells, with additional fluorescent puncta in the soma of hair cells (Fig. 8A inset). When saccular explants were incubated in ACM alone for 24 hours, the distinctive cytokeratin immunolabeling of the supporting cell apices is lost, and bright puncta are observed throughout the sensory epithelium, with somatic labeling within the sensory epithelium (Fig. 8B). Higher resolution imaging of these explants reveal cytokeratin immunolabeling of round (hair cell) apices compared to adjacent supporting cells, with bright punctate labeling associated with the hair bundle (Fig. 1B, 8B). When saccular explants were treated with gentamicin for 6 hours and allowed to recover in ACM for 18 hours, discrete cytokeratin immunolabeling occurs in round hair cell apices (Fig. 8C). When a hair cell extrusion occurs, intense cytokeratin labeling is observed (Fig. 1, 8). In all explants, the transitional epithelium surrounding the sensory epithelium is consistently labeled, regardless of drug treatment (Fig. 8).

Cytokeratin-labeled hair cell extrusions were present in all explants treated with gentamicin (Fig. 9), though far less frequently observed in explants co-incubated with latrunculin A and cytochalasin D-treated explants. Phalloidin labeling for F-actin indicated the cell borders of supporting cells and hair cells with their stereociliary bundles. Hair cell extrusions were usually rotund cytokeratin-labeled structures above the sensory epithelium. For 2-D presentation, 3-D rotations of stacks containing hair cell extrusions are shown in Figure 9. Numerous fluorescent speckles were also observed above the sensory epithelia (Fig. 9), despite extensive washing of explants, that were not present in situ preparations (data not shown). In addition to hair cell extrusions in colchicine and cytochalasin-treated explants after gentamicin treatment, cytokeratin labeling was also seen in fine protrusions from supporting cells that can also be identified in 3-D rotations (Fig. 10) that can also be seen in LM sections of cytochalasin D-treated explants (Fig. 7H).

Hair cell extrusions: transmission electron microscopy

In transmission electron micrographs of cross-sectioned saccular explants treated with gentamicin only, scar formations could frequently be identified below extruded cellular material above the sensory epithelium (Fig. 11). Beneath the extruded material, expanded apices of supporting cells with islands of electron-dense microfilamentous material were observed at the cell apex near the luminal membrane of the cell (Fig. 11B,C). At the supporting cell-supporting cell interface, junctional complexes (including tight junctions) were observed (Fig. 11B,C). The cell bodies of supporting cells participating in scar formations were often adjacent to one another, rather than separated by a hair cell body (Fig. 11B,C). Surviving hair cells contained electron-dense multi-vesiculated “gentamicin” bodies (Fig. 11B,C), similar to those previously described (Houghton et al., 1978;Toubeau et al., 1986) and not seen in control explants incubated in ACM (data not shown).

In cytochalasin D-treated explants (Fig. 11D), hair cells that survived drug administration appeared similar in density to hair cells in control (data not shown) and gentamicin-treated organs with well-defined stereocilia protruding from the cuticular plate (Fig. 11B,C). However, the soma of many hair cells was highly electron-translucent, with little cytoplasmic material beneath the luminal surface. The microfilamentous material of the junctional complexes in these translucent hair cell bodies were not visible, unlike those in adjacent supporting cell apices and those connecting surviving hair cells and their adjacent supporting cells (Fig. 11D). Within the cell body of the translucent hair cells were membrane-bound organelles, including the nucleus that was devoid of recognizable nuclear contents. The supporting cell apices adjacent to the translucent hair cells frequently had cytoplasmic and vacuolated protrusions into the extracellular space (Fig. 11D). The supporting cell apices did not expand into the spaces occupied by the hair cell apices (Fig. 11D) as observed in scar formations in sections of gentamicin treated-only explants (Fig. 11B,C).

Discussion

Cytoskeletal disruption agents had three levels of effect on bullfrog saccular explants treated with aminoglycosides. Microtubule disruption agents had no effect on hair cell extrusion or supporting cell scar formation. Myosin disruption agents appeared to slow down scar formation but not hair cell extrusion, while actin disruption agents blocked scar formation, and largely prevented the extrusion of dying hair cells. These effects and other data are discussed below.

Hair bundle density

Explantation caused a small but significant decrease in hair bundle (and presumptively, hair cell) density. Three cytoskeletal disruption agents (colchicine, ML-9, Y-27632) further decreased hair bundle density. In other culture models colchicine induced apoptosis in dentate

granule cells (Kim et al., 2002); ML-9 enhanced apoptosis in epithelial cell lines (Connell et al., 2006), and Y-27632 caused dose-dependent cell death in endothelial cells (Li et al., 2002). We assume these disruption agents cause similar apoptotic cell death mechanisms in hair cells *in vitro* as described for aminoglycosides induced apoptosis *in vitro* (Jiang et al., 2006b). However, neither microtubule nor myosin disruption agents prevented scar formation, demonstrating supporting cell viability. Treatment with actin disruption agents (cytochalasin D, latrunculin A) did not induce hair bundle loss over and above explantation trauma, and F-actin accumulation in supporting cell apices adjacent to missing hair bundles also demonstrate supporting cell viability. Cytochalasin D significantly shortened stereociliary length in euthermic rodent stereocilia over 24 hours (Rzadzinska et al., 2004), but did not appear to affect the stereocilia of surviving hair bundles in the poikilothermic bullfrogs. This suggests that amphibian stereociliary actin turnover is slower than in mammals, although detailed morphometric studies would be needed to verify this.

The addition of gentamicin always decreased hair bundle density. Since the intended effect was to induce hair cell death (whether by explantation, gentamicin, or other toxins), we could still test whether cytoskeletal disruption agents modulated hair cell extrusion and the cytoskeletal mechanisms involved in supporting cell scar formation.

Cytokeratins

In amphibian, avian and mammalian vestibular systems, cytokeratins are preferentially localized in supporting cells (Cyr et al., 2000; Meiteles et al., 1994; Stone et al., 1996). However, unlike previous studies, we also observed weak puncta of cytokeratin labeling in hair cells, possibly as a result of excision and otolithic membrane removal prior to fixation. Twenty four hours after explantation, we found widespread changes in cytokeratin expression in saccular epithelia, becoming more prevalent in hair cells than in supporting cells (Fig. 8). We also observed that *extruding* hair cells expressed intense cytokeratin labeling.

The antibody we used recognizes a conserved epitope present on bovine, human, avian (Gigi et al., 1982; Stone et al., 1996), and now amphibian cytokeratins, including polypeptides 10, 11, 18, and 19 (Moll et al., 1982). Cytokeratin pp 18 is expressed by apoptotic epithelial cells early in the cell death pathway (Leers et al., 1999). More generally, cytokeratin expression and its hyperphosphorylation is a characteristic by-product of apoptosis in epithelial cells and keratinocytes (Caulin et al., 1997; Grubauer et al., 1986; Ku et al., 1997; Li et al., 1995b). Cytokeratins (particularly pp 18 and 19) are also released into the extracellular space by apoptic cells (Sheard et al., 2002), which may account for the numerous puncta observed above the sensory epithelium in figure 8, figure 9 and figure 10.

Duncan et al (2006) reported an increase in fluorescence of unconventional myosins in extruding chick hair cells, and suggested that an increase in antigen availability due to loss of binding partners (reducing steric hindrance), or a pH-dependence of the fluorophore (apoptotic cells are more alkaline) may account for this increased labeling intensity. These hypotheses also apply to the increased cytokeratin labeling of extrusions over adjacent hair cells. However, the greatly increased cytokeratin labeling of surviving hair cells over those at timepoint 0, and the presence of luminal keratinous bodies suggest both synthesis and exocytosis of cytokeratins following explantation. *In toto*, this data suggests that explantation of bullfrog inner ear sensory epithelia from its *in vivo* fluid environment may push stressed hair cells into apoptotic cell death mechanisms. The loss of hair bundles following explantation alone supports this hypothesis.

Cytokeratin expression is down regulated during hair cell differentiation (Cyr et al., 2000; Raphael et al., 1987). The upregulation of cytokeratins in hair cells in hair cell extrusions

indicates the epithelial origin of these sensory cells, and associated apoptotic cell death mechanisms (Caulin et al., 1997; Leers et al., 1999).

Hair cell extrusion

Following noxious insult, hair cells are not always extruded from the sensory epithelium. Vestibular hair cells can cleave their apical mechanosensory apparatus, leaving the hair cell soma within the sensory epithelium. Many of these bundleless hair cells are subsequently phagocytosed (Gale et al., 2002), with a subsequent decrease in hair cell density. A few bundleless hair cells are capable of regenerating their apical mechanosensory apparatus (Gale et al., 2002), although not likely in the 24 hour timeframe used in this study. Thus, an extrusion from the sensory epithelium represents either ejection of the hair cell apex only, or the whole cell body. These extrusions, combined with subsequent supporting cell scar formations, are valid indicators of hair cell toxicity. In this study, extrusions were identified by intense cytokeratin labeling extending into the extracellular space, similar to that for myosin VI extruded avian hair cells (Duncan et al., 2006). Extruding amphibian hair cells did not present significant actin labeling (Fig. 1, Fig. 8, and Fig. 9) that might be expected in cleaved hair cell apices. Indeed, hair cell degeneration is accompanied by action depolymerization (Jiang et al., 2006a).

Actin disruption agents significantly interfered with frequency of hair cell extrusion, since many remnants of dead hair cells remained emplaced within the sensory epithelium, although the majority of their cytoplasmic and nuclear contents had dispersed. Thus, the involvement of dynamic actin processes appears to be required for hair cell extrusion. However, the mechanism that induces hair cell extrusion still remains unclear. One mechanism proposed has been that the supporting cells actively extrude the hair cell by expanding its somatic volume (Cotanche et al., 1990; Duncan et al., 2006). Our TEM evidence also shows a qualitative increase in soma area beneath a supporting cell scar (Fig 11). Acto-myosin contractile “purse string” cytoskeletal networks are required to extrude dying epithelial cells (Rosenblatt et al., 2001); however, such networks are not visible in the deeper lateral regions of vestibular supporting cells surrounding the peri-nuclear region of hair cells in this study or those of others (Gale et al., 2002; Meiteles et al., 1994)

Hair cell extrusion represents just one of several cell death pathways available to sensory hair cells, with necrosis, caspase-independent and classical apoptosis mechanisms also possible (Jiang et al., 2006b). The variety of cell death mechanisms suggests that multiple routes of toxicity induced by aminoglycosides (and other noxious insults) trigger a variety of different cell death pathways, of which extrusion is just one. Cytoskeletal disruption agents (particularly colchicine, ML-9 and Y-27632) could trigger additional cell death pathways to those induced by aminoglycosides, further obscuring our ability to identify the in vivo mechanisms of hair cell extrusion. Additionally, actin-disruption agents could interfere with the signalling interactions (e.g., cadherins, and catenins) between hair cells and supporting cells (Leonova et al., 1997; Warchol, 2002), to prevent hair cell extrusion, as well as expansion of the supporting cell apices into a scar formation,

Hair cell extrusion is also reminiscent of cellular blebbing processes seen in other tissues. Cellular shape changes (or type 1 blebs) are induced by microtubule-dissembling agents that dissociate the membrane from the cortical actin cytoskeleton of Walker carcinosarcoma cells (Keller et al., 1986). Small, possibly type I, blebs are seen in colchicine-treated explants (Fig. 10). Colchicine, which promotes microtubule depolymerization, may therefore adventitiously enhance hair cell extrusion as suggested by the significant drop in hair bundle density compared to explants treated without colchicine. However, if hair cell extrusion was dependent on the disassembly of microtubules, then taxol, an inhibitor of microtubule depolymerization would prevent hair cell extrusion, yet this did not occur. Thus, microtubule disruption agents do not

directly interfere with amphibian vestibular hair cell extrusion mechanisms, as hypothesized for mammalian vestibular hair cell extrusion (Li et al., 1995a).

Type 2 blebs are formed by the destruction of the cortical actin cytoskeleton by latrunculin A (Keller et al., 2002). Small blebs, or protrusions, occur at the apex of supporting cells of cytochalasin D- or latrunculin A-treated explants. In wholemounted explants that received actin-disruption agents, hair cell extrusions were rarely observed, and in sections of these same explants, extrusions were never seen. Instead, many translucent (dead) hair cells were observed within the sensory epithelium that and had lost their cellular integrity and composition. Thus dynamic actin networks are involved in the extrusion of the dying hair cell that is distinct from type II bleb formation.

Hair cell extrusion is not dependent on myosin-based cytoskeletal mechanisms, as myosin disruption agents appeared to only (qualitatively) slow down the rate of supporting cell scar closure (Fig 5), rather than hair cell extrusion. This is in contrast to the involvement of dynamic acto-myosin processes in the extrusion of apoptic MDCK cells in vitro (Rosenblatt et al., 2001).

Cell deformation (Type 3 blebs) can be induced by increased intracellular pressure (e.g., acto-myosin contractility), however, such cells tend to recover their original morphology (Schutz et al., 1998), unlike extruded hair cells. Intracellular pressure may contribute to hair cell extrusion, for example, depolymerization of F-actin, the cortical cytoskeleton and/or glycogenic stores may lead to an increase in osmolytes within the cell, drawing water into the cell and hence swelling (Jiang et al., 2006a; Zhi et al., 2007). In contrast, mammalian inner hair cell blebbing occurred in hyper-osmotic conditions *in vitro*, suggesting that intracellular pressure is not required (Shi et al., 2005). The direct mechanism that extrudes hair cell during the cell death process therefore remains to be determined.

Hair cell extrusion also occurs in avian basilar papilla (Cotanche et al., 1990; Duncan et al., 2006; Kil et al., 1997) and mammalian vestibular organs (Duvall et al., 1963; Lang et al., 1997; Li et al., 1995a), but not in mammalian cochlear sensory epithelia. Instead the outer hair cell body degenerates beneath the supporting cell scar formation (Forge, 1985; Raphael et al., 1991). OHCs are unique, in that their lateral membranes are not in contact with adjacent cells. Thus, there maybe no external supporting cells pressure to eject OHCs from the sensory epithelium as postulated for vestibular and non-mammalian hair cells (Cotanche et al., 1990). Instead, the OHC apex is cleaved from the OHC soma by the expanding supporting cell processes (Forge, 1985; Leonova et al., 1997). The OHC soma is likely phagocytosed by adjacent supporting cells as it disintegrates (Abrashkin et al., 2006), reminiscent of the removal of many bundleless hair cells by macrophages in amphibian sensory epithelia (Gale et al., 2002). Little analogous research has been published on the cellular degeneration of inner hair cells following noxious insult.

Closure of supporting cell scar formations

Supporting cell scar formations display a characteristic multi-cellular actin ring/cartwheel illustrated by the F-actin labeled spokes (Steyger et al., 1997). As the hair cell (apex) is extruded, the adjacent actiniferous junctional complexes of supporting cells initially remain within the cytoplasm, but no longer attached to the baso-lateral membrane that has now extended from the original cell border to encompass the expanded supporting cell apex participating in the scar formation, as described previously for mammalian vestibular sensory epithelia (Meiteles et al., 1994). This “ring” is likely to be analogous to the isolated patches of microfilamentous material within the apices of supporting cells in transmission electron microscopy cross-sections of scar formations that are unassociated with the plasma membrane. Such isolated patches of microfilamentous material are not seen in the apices of supporting

cells not participating in scar formations. These multi-cellular actin rings/cartwheels are transient structures as the junctional complexes of the former supporting cell boundary (the “ring”) are likely dissembled over time. These multi-cellular actin rings are occur less frequently in sensory epithelia allowed to recover for several days after cytotoxic insult in explants that show a drop in hair bundle density (Steyger et al., 1997).

Microtubule disruption agents did not prevent supporting cell scar formation. Colchicine blocks the polymerization of microtubules, promoting microtubular disassembly (Bergen et al., 1983; Platts et al., 1999), inducing actin polymerization (Jung et al., 1997). The cortical microtubular cytoskeleton is essential for accurate deposition of F-actin (Dent et al., 2001; Mandato et al., 2003; Rodriguez et al., 2003; Vasiliev et al., 1970). Thus, the enhanced deposition of F-actin within the center of expanded supporting cell apices in colchicine-treated explants may represent a build-up of F-actin that is not properly integrated into the cortical actin cytoskeleton due to the inability of the cortical microtubular network to extend (polymerize) into the expanding supporting cell apex. Nonetheless, the supporting cell apices are still able to expand, and form junctional complexes, demonstrating that microtubule polymerization is not essential for cell expansion and supporting cell scar formation. Indeed, there is evidence that microtubular depolymerization can accelerate wound closure (Bement et al., 1999; Rodriguez et al., 2003).

The inaccurate deposition of F-actin in colchicine-treated explants is not seen in expanded supporting cell apices in taxol-treated explants. Taxol blocks microtubule depolymerization, but allows polymerization (Arnal et al., 1995; Kumar, 1981). Thus, the cortical microtubular cytoskeleton is able to extend in synchrony with the cell membrane, as the supporting cell apices close the breech in the sensory epithelium, enabling appropriate deposition of F-actin at the cell border (Mandato et al., 2003).

Unlike microtubule inhibitors, the actin inhibitors latrunculin A and cytochalasin D had a profound impact on the expansion of supporting cell apices participating in the scar formations. Cytochalasin D and latrunculin A both block the polymerization of actin, while allowing F-actin depolymerization to proceed (Brenner et al., 1979; Casella et al., 1981; Coue et al., 1987; Morton et al., 2000). Thus, the expansion of supporting cell apices appears to be dependent upon a net polymerization of cortical F-actin networks, potentially triggered by specific signals from extruding hair cells, as in MDCK cells (Rosenblatt et al., 2001).

Cytochalasin D allows some F-actin polymerization, unlike latrunculin A (Brenner et al., 1979; Morton et al., 2000). This may account for the extra deposition of F-actin at the confluence of two supporting cell apices adjacent to dead, dying or missing hair cells (Fig. 6). The ability for the supporting cell apices to physically expand may be dependent on the release of the apical tight and adherens junctions, perhaps by β-catenin and cadherin interactions between hair cells and their surrounding supporting cells (Gale et al., 2002; Warchol, 2002). EM examination of cytochalasin D explants reveals that the hair cell contribution to the junctional complex is absent. However, supporting cells remain unable to expand into the hair cell space, suggesting that actin disruption agents interfere with hair cell-supporting cell signaling. Blebbing by supporting cells adjacent to emplaced, translucent hair cells may be type II blebs that occur following cytochalasin D and latrunculin A treatment in other cell systems (Keller et al., 1986), and recovery of explants in the absence of these disruption agents may reduce the frequency and extent of blebbing. Indeed, blebbing was generally not observed in our control or gentamicin-treated only explants 24 hours after explantation.

Since acto-myosin “purse-string” contractions are necessary for epithelial cell wound closure (Bement et al., 1999; Rosenblatt et al., 2001), we hypothesized that myosin disruption agents would also prevent scar formation, and leave open lesions as did actin disruption agents.

Instead, we frequently found both partially-closed and fully-closed supporting cell scar formations in explants treated with myosin disruption agents suggesting that the expansion of the supporting cell apices has been decelerated. We rarely saw partially-closed scar formations in explants treated without myosin disruption agents. However, despite disruption of myosin function, scar formation occurs but at much slower rate, perhaps assisted by actin polymerization and microtubules (Dent et al., 2001). This hypothesis is supported by the negligible or weak labeling for F-actin by phalloidin within the scar formation compared to the equivalent intensity and breadth of actin labeling in scar formations and adjacent supporting cells in other explants, perhaps due to reduced acto-myosin cortical flow of cytoplasm (Rodriguez et al., 2003). Alternatively, though less likely, the myosin disruption agents were not sufficiently specific for the potential range of myosin and their regulatory units expressed in supporting cells; thus functional redundancy may enable closure of expanding supporting cell apices, albeit at an impaired rate. Nonetheless, the involvement of myosin is essential for sealing the breach in the epithelium in a timely matter, as shown in other systems (Bement, 2002; Bement et al., 1999; Rosenblatt et al., 2001). It would be interesting to test the effect of combined treatment with myosin and microtubule disruption agents on supporting cell scar formation.

The sealing of the potential breach in sensory epithelia is necessary to prevent the admixture of endolymphatic and perilymphatic fluids, thereby maintaining the endolymphatic potential and sensitive hair cell function (Forge, 1985; Meiteles et al., 1994; Steel, 1999). Despite significant challenges to the microtubule and myosin components of their cytoskeleton, supporting cells were still able to seal the epithelial barrier in a manner reminiscent of the cytoarchitectural reorganization of supporting cells in the original classical descriptions using rodents (Forge, 1985; Meiteles et al., 1994; Raphael, 1992; Raphael, 1993; Raphael et al., 1991). Thus, there are strong similarities in the closure of hair cell lesions across phyla. The disruption of the filamentous actin network, largely by depolymerization, and/or filament polymerization, further emphasizes the significant role played by actin cytoskeleton in wound closure, and the development of junctional complexes (Rodriguez et al., 2003).

Although hair cell extrusion and supporting cell scar formation require dynamic actin activity, the exact mechanism by which hair cells are extruded from the sensory epithelium requires further investigation. A better understanding of mechanisms that prevent supporting cell scar formation that maintain an anatomically-disrupted sensory epithelium immediately after noxious insult may provide another avenue for hair cell progenitors to integrate into the sensory epithelium (Li et al., 2003) without gross, mechanical lesions.

Acknowledgements

Funded by NIDCD R01 4555 (PSS), 04555s (AJH); P30 05983 and by the Oregon Lions Sight and Hearing Foundation. The authors thank Dennis Trune, Huy Bui and Juany Rehling for assistance with transmission light and electron microscopy, and Takatoshi Karasawa for comments on the manuscript.

References

Abrashkin KA, Izumikawa M, Miyazawa T, Wang CH, Crumling MA, Swiderski DL, Beyer LA, Gong TW, Raphael Y. The fate of outer hair cells after acoustic or ototoxic insults. Hear Res 2006;218:20–29. [PubMed: 16777363]

Arnal I, Wade RH. How does taxol stabilize microtubules? Curr Biol 1995;5:900–908. [PubMed: 7583148]

Baird RA, Steyger PS, Schuff NR. Mitotic and nonmitotic hair cell regeneration in the bullfrog vestibular otolith organs. Ann N Y Acad Sci 1996;781:59–70. [PubMed: 8694449]

Bement WM. Actomyosin rings: the riddle of the sphincter. Curr Biol 2002;12:R12–R14. [PubMed: 11790316]

Bement WM, Mandato CA, Kirsch MN. Wound-induced assembly and closure of an actomyosin purse string in Xenopus oocytes. Curr Biol 1999;9:579–587. [PubMed: 10359696]

Bergen LG, Borisy GG. Tubulin-colchicine complex inhibits microtubule elongation at both plus and minus ends. J Biol Chem 1983;258:4190–4194. [PubMed: 6833250]

Brenner SL, Korn ED. Substoichiometric concentrations of cytochalasin D inhibit actin polymerization. Additional evidence for an F-actin treadmill. J Biol Chem 1979;254:9982–9985. [PubMed: 489616]

Brown BK, Song W, et al. The actin cytoskeleton is required for the trafficking of the B cell antigen receptor to the late endosomes. Traffic 2001;2:414–427. [PubMed: 11389769]

Casella JF, Flanagan MD, Lin S. Cytochalasin D inhibits actin polymerization and induces depolymerization of actin filaments formed during platelet shape change. Nature 1981;293:302–305. [PubMed: 7196996]

Caulin C, Salvesen GS, Oshima RG. Caspase cleavage of keratin 18 and reorganization of intermediate filaments during epithelial cell apoptosis. J Cell Biol 1997;138:1379–1394. [PubMed: 9298992]

Connell LE, Helfman DM. Myosin light chain kinase plays a role in the regulation of epithelial cell survival. J Cell Sci 2006;119:2269–2281. [PubMed: 16723733]

Cotanche DA, Dopyera CE. Hair cell and supporting cell response to acoustic trauma in the chick cochlea. Hear Res 1990;46:29–40. [PubMed: 2380125]

Coue M, Brenner SL, Spector I, Korn ED. Inhibition of actin polymerization by latrunculin A. FEBS Lett 1987;213:316–318. [PubMed: 3556584]

Cyr JL, Bell AM, Hudspeth AJ. Identification with a recombinant antibody of an inner-ear cytokeratin, a marker for hair-cell differentiation. Proc Natl Acad Sci U S A 2000;97:4908–4913. [PubMed: 10758152]

Dent EW, Kalil K. Axon branching requires interactions between dynamic microtubules and actin filaments. J Neurosci 2001;21:9757–9769. [PubMed: 11739584]

Duncan LJ, Mangiardi DA, Matsui JI, Anderson JK, McLaughlin-Williamson K, Cotanche DA. Differential expression of unconventional myosins in apoptotic and regenerating chick hair cells confirms two regeneration mechanisms. J Comp Neurol 2006;499:691–701. [PubMed: 17048225]

Duncan RK, Ile KE, Dubin MG, Saunders JC. Hair bundle profiles along the chick basilar papilla. J Anat 2001;198:103–116. [PubMed: 11215761]

Duvall AJ, Wersall J. Site of action of streptomycin upon inner ear sensory cells. Acta Otolaryngol 1963;57:581–598. [PubMed: 14181104]

Forge A. Outer hair cell loss and supporting cell expansion following chronic gentamicin treatment. Hear Res 1985;19:171–182. [PubMed: 4055536]

Gale JE, Meyers JR, Periasamy A, Corwin JT. Survival of bundleless hair cells and subsequent bundle replacement in the bullfrog's saccule. J Neurobiol 2002;50:81–92. [PubMed: 11793356]

Gigi O, Geiger B, Eshhar Z, Moll R, Schmid E, Winter S, Schiller DL, Franke WW. Detection of a cytokeratin determinant common to diverse epithelial cells by a broadly cross-reacting monoclonal antibody. Embo J 1982;1:1429–1437. [PubMed: 6202509]

Grubauer G, Romani N, Kofler H, Stanzl U, Fritsch P, Hintner H. Apoptotic keratin bodies as autoantigen causing the production of IgM- anti-keratin intermediate filament autoantibodies. J Invest Dermatol 1986;87:466–471. [PubMed: 2428883]

Houghton DC, Campbell-Boswell MV, Bennett WM, Porter GA, Brooks RE. Myeloid bodies in the renal tubules of humans: relationship to gentamicin therapy. Clin Nephrol 1978;10:140–145. [PubMed: 719967]

Humes HD. Insights into ototoxicity. Analogies to nephrotoxicity. Ann N Y Acad Sci 1999;884:15–18. [PubMed: 10842580]

Jiang H, Sha SH, Schacht J. Rac/Rho pathway regulates actin depolymerization induced by aminoglycoside antibiotics. J Neurosci Res 2006a;83:1544–1551. [PubMed: 16521128]

Jiang H, Sha SH, Forge A, Schacht J. Caspase-independent pathways of hair cell death induced by kanamycin in vivo. Cell Death Differ 2006b;13:20–30. [PubMed: 16021180]

Jung HI, Shin I, Park YM, Kang KW, Ha KS. Colchicine activates actin polymerization by microtubule depolymerization. Mol Cells 1997;7:431–437. [PubMed: 9264034]

Keller H, Rentsch P, Hagmann J. Differences in cortical actin structure and dynamics document that different types of blebs are formed by distinct mechanisms. Exp Cell Res 2002;277:161–172. [PubMed: 12083798]

Keller HU, Zimmermann A. Shape changes and chemokinesis of Walker 256 carcinosarcoma cells in response to colchicine, vinblastine, nocodazole and taxol. Invasion Metastasis 1986;6:33–43. [PubMed: 2867063]

Kil J, Warchol ME, Corwin JT. Cell death, cell proliferation, and estimates of hair cell life spans in the vestibular organs of chicks. Hear Res 1997;114:117–126. [PubMed: 9447926]

Kim JA, Mitsukawa K, Yamada MK, Nishiyama N, Matsuki N, Ikegaya Y. Cytoskeleton disruption causes apoptotic degeneration of dentate granule cells in hippocampal slice cultures. Neuropharmacology 2002;42:1109–1118. [PubMed: 12128012]

Ku NO, Liao J, Omary MB. Apoptosis generates stable fragments of human type I keratins. J Biol Chem 1997;272:33197–33203. [PubMed: 9407108]

Kumar N. Taxol-induced polymerization of purified tubulin. Mechanism of action. J Biol Chem 1981;256:10435–10441. [PubMed: 6116707]

Lang H, Liu C. Apoptosis and hair cell degeneration in the vestibular sensory epithelia of the guinea pig following a gentamicin insult. Hear Res 1997;111:177–184. [PubMed: 9307323]

Leers MP, Kolgen W, Bjorklund V, Bergman T, Tribbick G, Persson B, Bjorklund P, Ramaekers FC, Bjorklund B, Nap M, Jornvall H, Schutte B. Immunocytochemical detection and mapping of a cytokeratin 18 neo-epitope exposed during early apoptosis. J Pathol 1999;187:567–572. [PubMed: 10398123]

Leonova EV, Raphael Y. Organization of cell junctions and cytoskeleton in the reticular lamina in normal and ototoxically damaged organ of Corti. Hear Res 1997;113:14–28. [PubMed: 9387983]

Li H, Roblin G, Liu H, Heller S. Generation of hair cells by stepwise differentiation of embryonic stem cells. Proc Natl Acad Sci U S A 2003;100:13495–13500. [PubMed: 14593207]

Li L, Nevill G, Forge A. Two modes of hair cell loss from the vestibular sensory epithelia of the guinea pig inner ear. J Comp Neurol 1995a;355:405–417. [PubMed: 7636022]

Li L, Tucker RW, Hennings H, Yuspa SH. Chelation of intracellular Ca2+ inhibits murine keratinocyte differentiation in vitro. J Cell Physiol 1995b;163:105–114. [PubMed: 7896886]

Li X, Liu L, Tupper JC, Bannerman DD, Winn RK, Sebti SM, Hamilton AD, Harlan JM. Inhibition of protein geranylgeranylation and RhoA/RhoA kinase pathway induces apoptosis in human endothelial cells. J Biol Chem 2002;277:15309–15316. [PubMed: 11839765]

Mandato CA, Bement WM. Actomyosin transports microtubules and microtubules control actomyosin recruitment during Xenopus oocyte wound healing. Curr Biol 2003;13:1096–1105. [PubMed: 12842008]

Meiteles LZ, Raphael Y. Scar formation in the vestibular sensory epithelium after aminoglycoside toxicity. Hear Res 1994;79:26–38. [PubMed: 7528737]

Miller, JJ. Handbook of ototoxicity. Boca Raton: CRC Press; 1985.

Moll R, Franke WW, Schiller DL, Geiger B, Krepler R. The catalog of human cytokeratins: patterns of expression in normal epithelia, tumors and cultured cells. Cell 1982;31:11–24. [PubMed: 6186379]

Morton WM, Ayscough KR, McLaughlin PJ. Latrunculin alters the actin-monomer subunit interface to prevent polymerization. Nat Cell Biol 2000;2:376–378. [PubMed: 10854330]

Pillers DA, Kempton JB, Duncan NM, Pang J, Dwinnell SJ, Trune DR. Hearing loss in the laminin-deficient dy mouse model of congenital muscular dystrophy. Mol Genet Metab 2002;76:217–224. [PubMed: 12126936]

Platts SH, Falcone JC, Holton WT, Hill MA, Meininger GA. Alteration of microtubule polymerization modulates arteriolar vasomotor tone. Am J Physiol 1999;277:H100–H106. [PubMed: 10409187]

Raphael Y. Evidence for supporting cell mitosis in response to acoustic trauma in the avian inner ear. J Neurocytol 1992;21:663–671. [PubMed: 1403011]

Raphael Y. Reorganization of the chick basilar papilla after acoustic trauma. J Comp Neurol 1993;330:521–532. [PubMed: 8320342]

Raphael Y, Altschuler RA. Reorganization of cytoskeletal and junctional proteins during cochlear hair cell degeneration. Cell Motil Cytoskeleton 1991;18:215–227. [PubMed: 1711932]

Raphael Y, Marshak G, Barash A, Geiger B. Modulation of intermediate-filament expression in developing cochlear epithelium. Differentiation 1987;35:151–162. [PubMed: 2450800]

Rodriguez OC, Schaefer AW, Mandato CA, Forscher P, Bement WM, Waterman-Storer CM. Conserved microtubule-actin interactions in cell movement and morphogenesis. Nat Cell Biol 2003;5:599–609. [PubMed: 12833063]

Rosenblatt J, Raff MC, Cramer LP. An epithelial cell destined for apoptosis signals its neighbors to extrude it by an actin- and myosin-dependent mechanism. Curr Biol 2001;11:1847–1857. [PubMed: 11728307]

Rzadzinska AK, Schneider ME, Davies C, Riordan GP, Kachar B. An actin molecular treadmill and myosins maintain stereocilia functional architecture and self-renewal. J Cell Biol 2004;164:887–897. [PubMed: 15024034]

Schutz K, Keller H. Protrusion, contraction and segregation of membrane components associated with passive deformation and shape recovery of Walker carcinosarcoma cells. Eur J Cell Biol 1998;77:100–110. [PubMed: 9840459]

Sheard MA, Vojtesek B, Simickova M, Valik D. Release of cytokeratin-18 and -19 fragments (TPS and CYFRA 21-1) into the extracellular space during apoptosis. J Cell Biochem 2002;85:670–677. [PubMed: 11968007]

Shi X, Gillespie PG, Nuttall AL. Na+ influx triggers bleb formation on inner hair cells. Am J Physiol Cell Physiol 2005;288:C1332–C1341. [PubMed: 15689412]

Steel KP. Perspectives: biomedicine. The benefits of recycling. Science 1999;285:1363–1364. [PubMed: 10490411]

Steyger PS, Gillespie PG, Baird RA. Myosin Ibeta is located at tip link anchors in vestibular hair bundles. J Neurosci 1998;18:4603–4615. [PubMed: 9614235]

Steyger PS, Burton M, Hawkins JR, Schuff NR, Baird RA. Calbindin and parvalbumin are early markers of non-mitotically regenerating hair cells in the bullfrog vestibular otolith organs. Int J Dev Neurosci 1997;15:417–432. [PubMed: 9263023]

Stone JS, Leano SG, Baker LP, Rubel EW. Hair cell differentiation in chick cochlear epithelium after aminoglycoside toxicity: in vivo and in vitro observations. J Neurosci 1996;16:6157–6174. [PubMed: 8815898]

Toubeau G, Maldague P, Laurent G, Vaamonde CA, Tulkens PM, Heuson-Stiennon JA. Morphological alterations in distal and collecting tubules of the rat renal cortex after aminoglycoside administration at low doses. Virchows Arch B Cell Pathol Incl Mol Pathol 1986;51:475–485. [PubMed: 2878521]

Vasiliev JM, Gelfand IM, Domnina LV, Ivanova OY, Komm SG, Olshevskaja LV. Effect of colcemid on the locomotory behaviour of fibroblasts. J Embryol Exp Morphol 1970;24:625–640. [PubMed: 4923996]

Warchol ME. Cell density and N-cadherin interactions regulate cell proliferation in the sensory epithelia of the inner ear. J Neurosci 2002;22:2607–2616. [PubMed: 11923426]

Wolf E, Quimby MC. Amphibian cell culture: permanent cell line from the bullfrog (*Rana catesbeiana*). Science 1964;144:1578–1580. [PubMed: 14169344]

Zhi M, Ratnanather JT, Ceyhan E, Popel AS, Brownell WE. Hypotonic swelling of salicylate-treated cochlear outer hair cells. Hearing Research. 2007(in press)

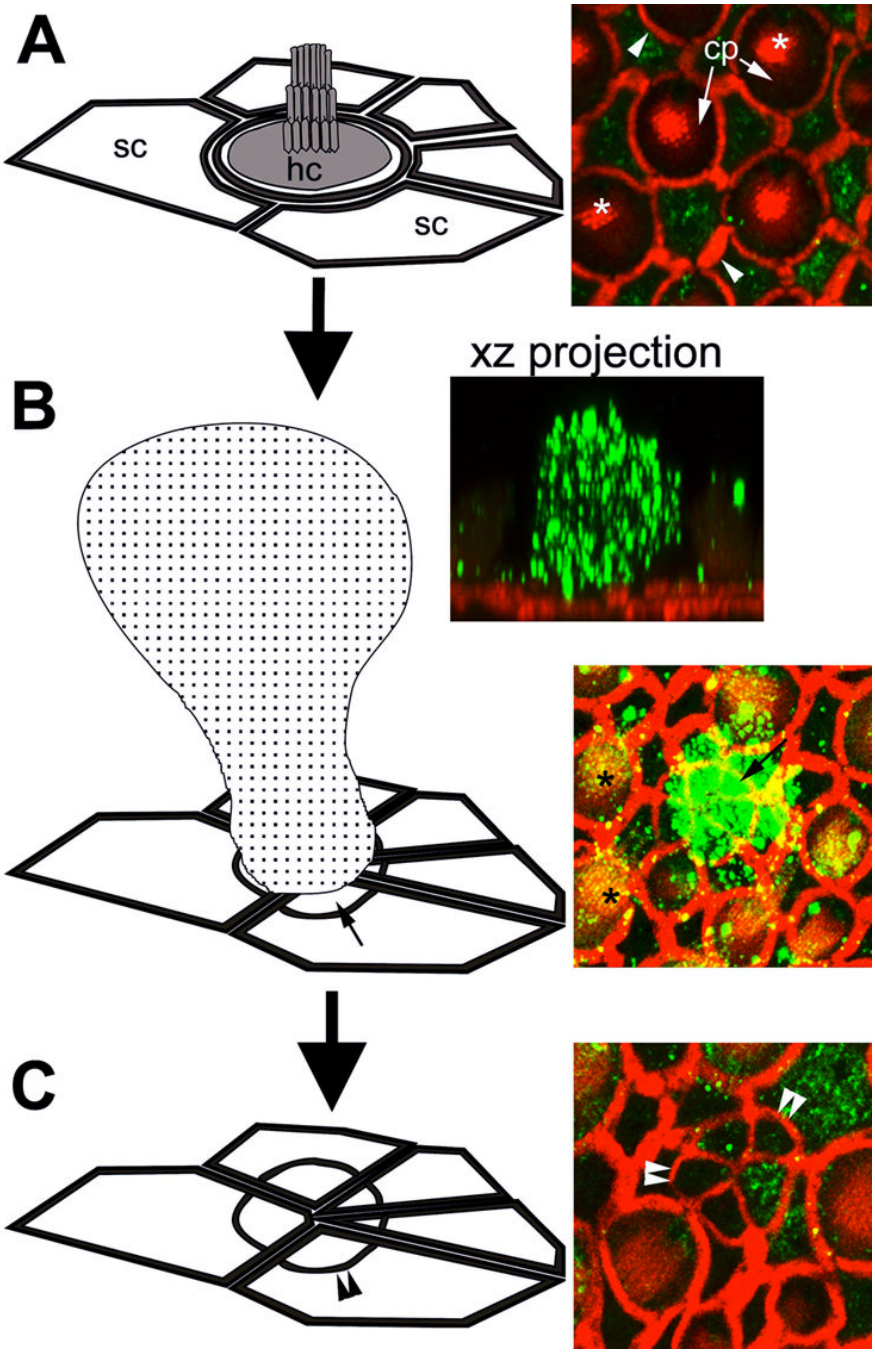

Figure 1.

The morphogenesis of a scar formation. (A) Each saccular hair cell (hc) is surrounded by as many as 6 supporting cells (sc), characterized by their polygonal apical surfaces. In the micrograph on the right, actin (red) labels the actiniferous junctional complexes between adjacent cells (arrowheads), the cuticular plate (cp) and hair bundle (*) (shown in the schematic as shaded regions). Cytokeratins (green) are largely localized in the supporting cells, although some expression in hair cells can be seen surrounding the cuticular plate. (B) The extrusion of a dying hair cell (speckled cell in schematic) correlates with extensive cytokeratin expression within extruded hair cell body (green) in an xz projection. The surrounding supporting cells expand their apical processes (small arrows) to seal the surface of the sensory epithelium,

beneath the extruded hair cell. This produces a supporting cell scar formation (C), characterized by a multi-cellular actin ring (double arrowheads). Note the cytokeratin expression (green) within the supporting cell scar. Note also the punctate cytokeratin labeling (yellow-green) associated with hair bundles (*) in (B). A: in situ; B and C 24 hours after explantation. (Not to scale, for illustrative purposes only.)

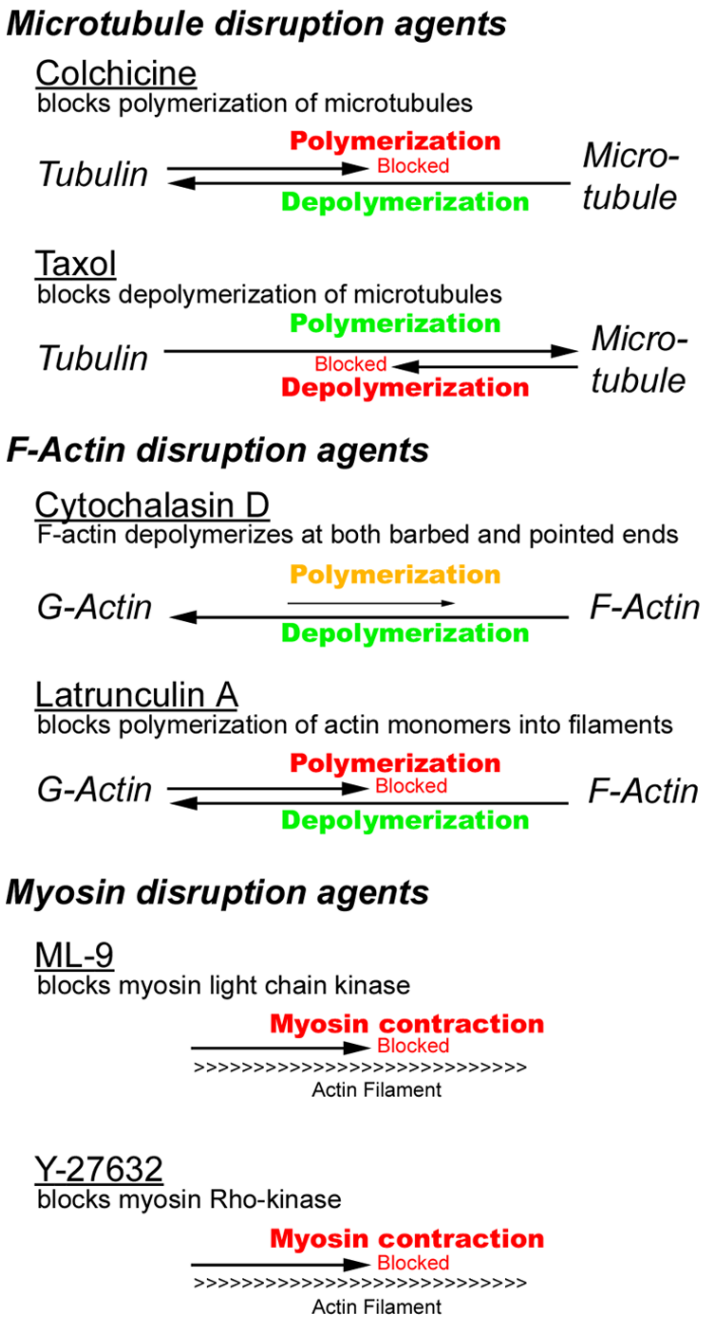

Figure 2.
Schematic representation of the effects of specific cytoskeletal disruption agents.

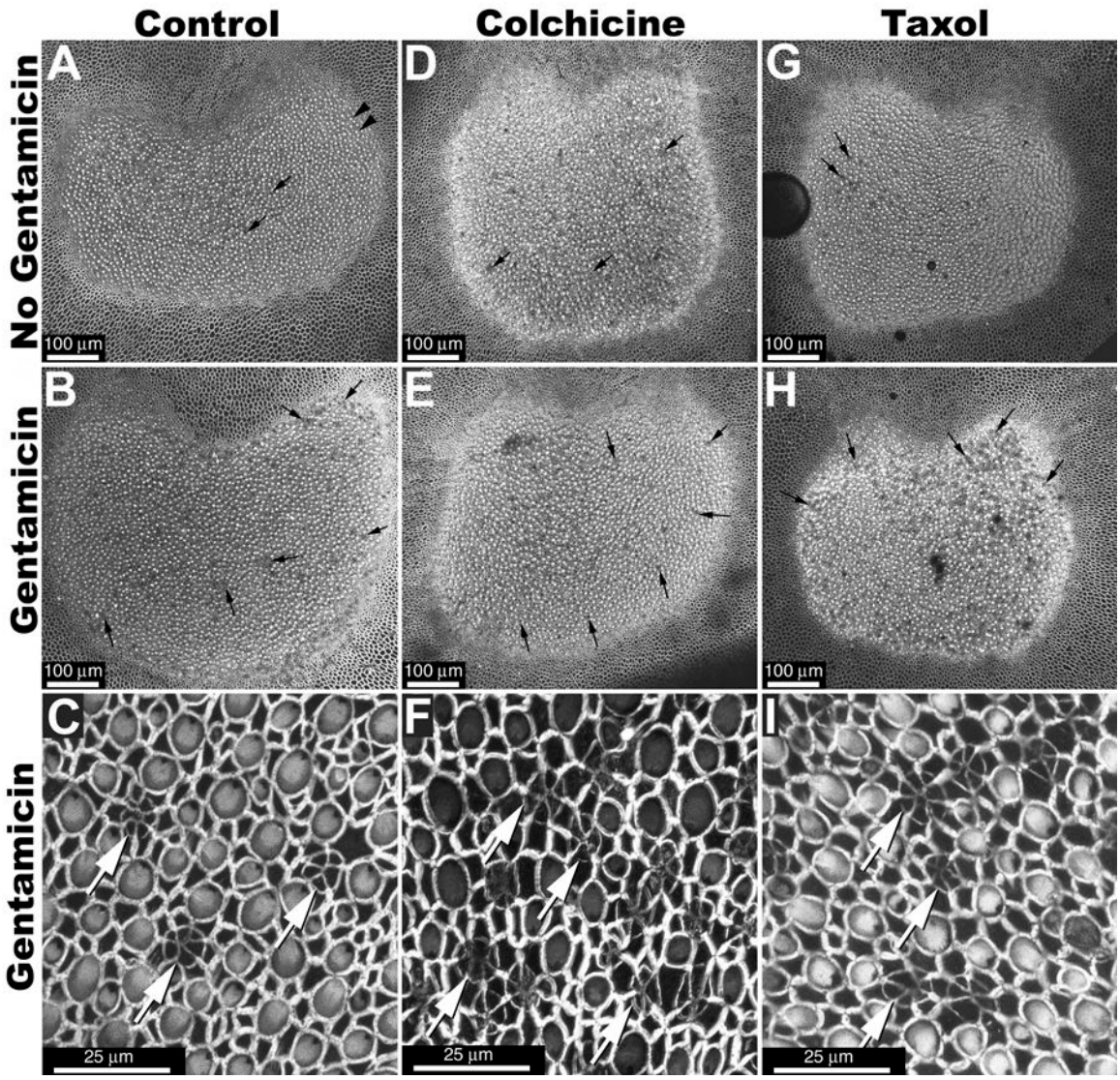

Figure 3.

(A) When whole-mounted control saccular explants (incubated in ACM only for 24 hours) are viewed perpendicular to the luminal surface at low magnification, hair bundles appear as intensely fluorescent dots (arrowheads). Regions with missing hair bundles can also be identified (small arrows), and are more frequent in explants treated with gentamicin (B) or with gentamicin plus microtubule disruption agents (E, H) compared to non-gentamicin-treated control explants (A,D,G). (C, F, I) High resolution imaging of the sensory epithelium reveals characteristic multi-cellular rings/cartwheels of labeled actin (white arrows) at the site of missing hair bundles. Scale bars in µm.

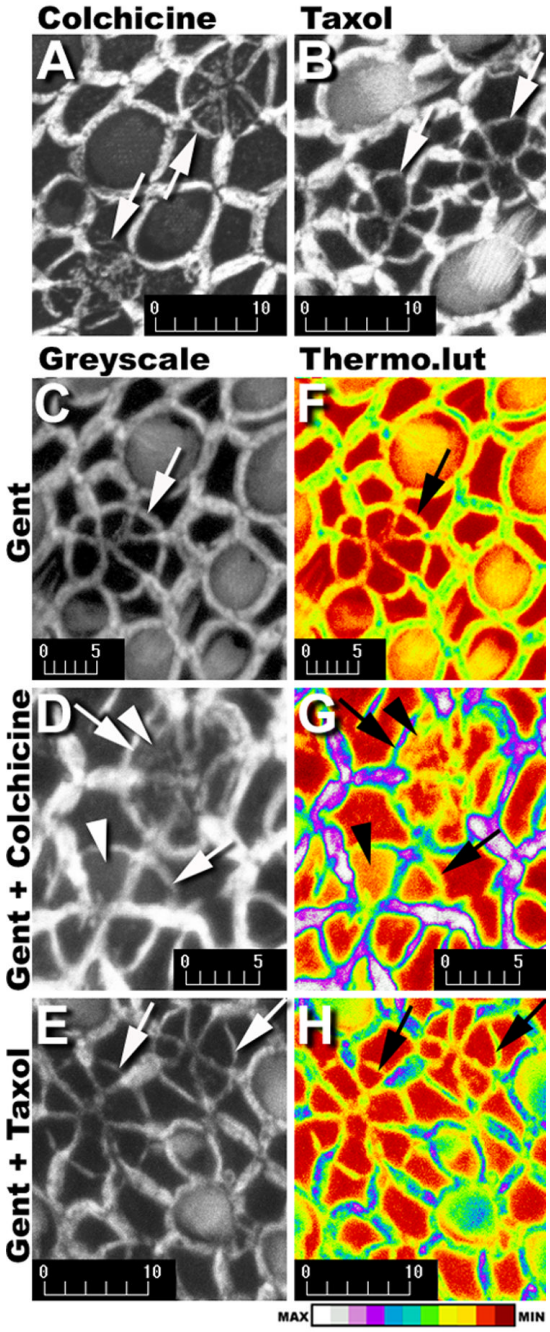

Figure 4.

Phalloidin-labeled multicellular rings/cartwheels (↑) in explants treated with gentamicin plus colchicine (A) or gentamicin plus taxol (B). In colchicine-treated explants (A, D), deposition of F-actin (arrowhead) occurs within the expanded apical processes of supporting cells participating in the scar formation, but not in scar formations of gentamicin treated (C), or gentamicin plus taxol-treated explants (B,E). When the grayscale images in C–E are loaded with the Thermo look-up table (F–H), a dark red indicates the absence of phalloidin-conjugated Alexa 568 fluorescence, and white represents maximum fluorescence intensity (see intensity bar at bottom). Supporting cell apices not participating in scar formations in all explants (F–H), are red or dark red. Colchicine-treated explants (G) have yellow pixels within the central

region of the expanded supporting cell apices participating in scar formations (arrowheads) in contrast to the dark red pixels throughout the scar formations in explants treated with gentamicin only (F) or gentamicin plus taxol (H). Scale bars in microns.

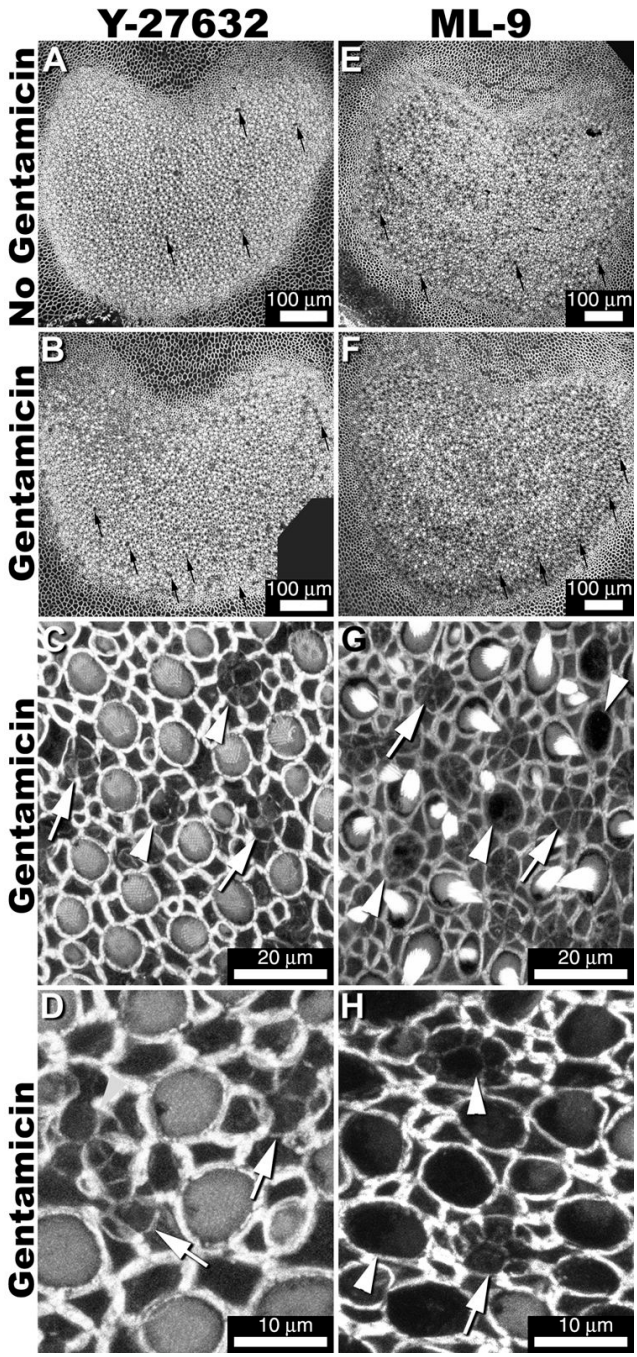

Figure 5.

Low resolution images of explants treated with myosin disruption agents Y-27632 (A) or ML-9 (E) reveal hair bundle loss (small arrows). Explants treated with these myosin disruption agents plus gentamicin (B,F) show greater hair bundle loss compared to myosin disruption agent treatment only (A,E). High resolution imaging of explants treated with Y-27632 (C,D) or ML-9 (F,H) show a mix of closed scar formations (arrows), and partially-closed scar formations (arrowheads). Some closed scars appeared weakly-fluorescent and structurally disorganized (D,H arrow). Partially-closed scars have little fluorescence at the leading edges of newly-expanding supporting cell apical processes (G,H).

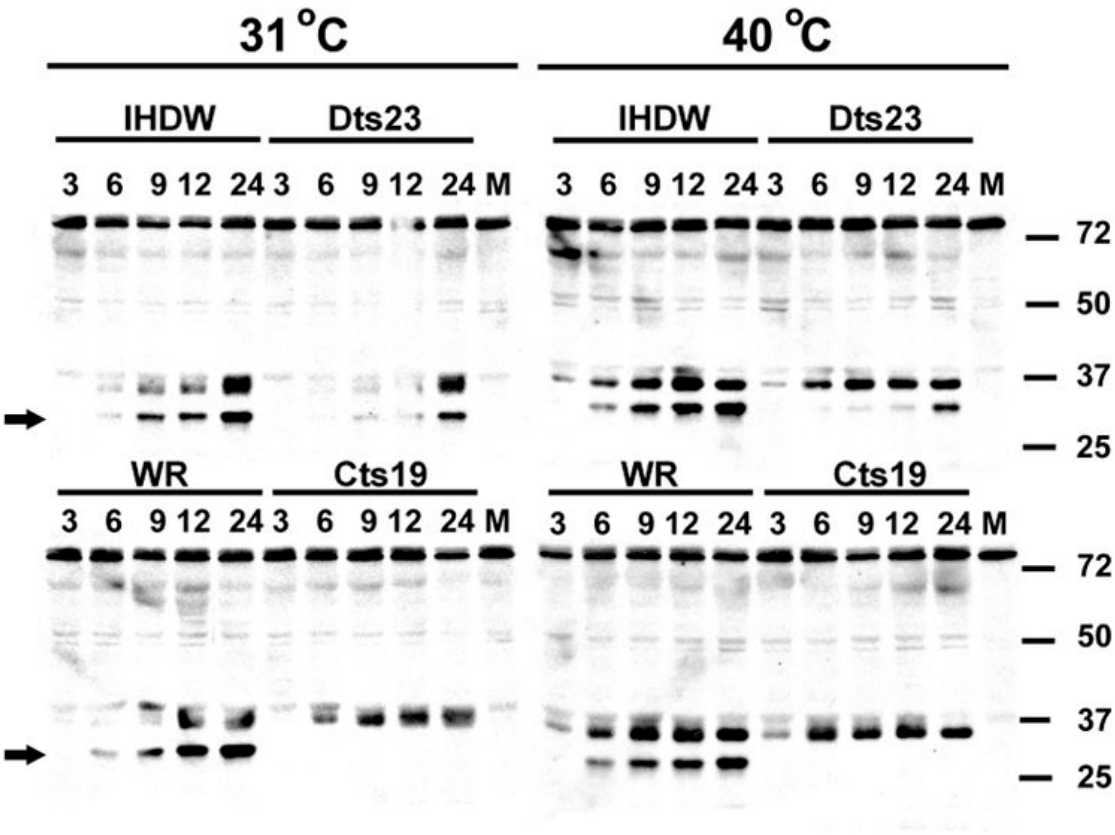

Figure 6.

At low magnification, phalloidin-labeled explants treated with actin disruption agents – cytochalasin D (A) and Latrunculin A (E) contain fewer missing hair bundles compared to explants treated with both gentamicin and actin disruption agents only (B,F). High magnification imaging of regions containing missing hair cells (C,D,G,H) show dark circular or ovoid areas in the sensory epithelium. (C) A projection of F-actin phalloidin labeling of hair cell lesions in a cytochalasin D-treated explant. (D) A single optical section from the projection shown in (D), with intense fluorescence for F-actin (arrows) at the junctional confluences between two supporting cells (arrows in C). (G) Projection of hair cell lesions in latrunculin A-treated explants. (H) A single optical section from the projection shown in (G), that does not show intense F-actin phalloidin labeling (arrows) at the junctional confluences between two supporting cells (arrows in G).

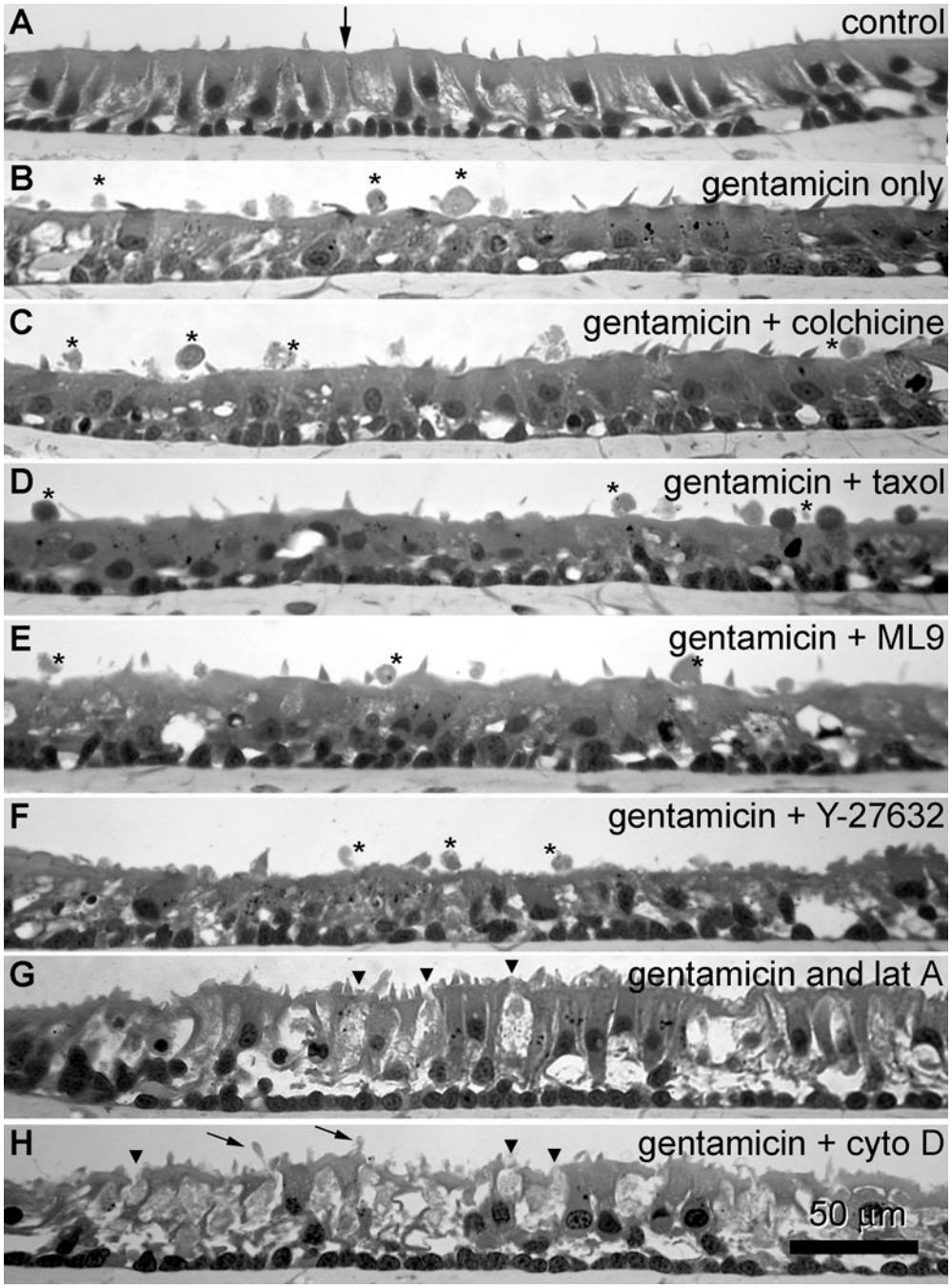

Figure 7.

(A) After incubation in ACM alone for 24 hours, cellular extrusions are not observed above the sensory epithelium in sections of explants embedded in methacrylate. (B) In sections from explants fixed 18 hours after a 6-hour incubation with gentamicin, cellular extrusions (*) are frequently seen above the sensory epithelium. Sections from explants co-incubated with gentamicin plus colchicine (C), taxol (D), ML-9 (E) or Y-27632 (F) also frequently had extrusions (*) above the sensory epithelium. Sections from explants treated with gentamicin plus latrunculin A (G) or cytochalasin D (H) did not display cellular extrusions, and had numerous translucent hair cell bodies (arrowheads) embedded within the sensory epithelium. In addition, explants treated with gentamicin plus cytochalasin D, fine protrusions of cellular

material (small arrows) can be seen extending from supporting cells into the extracellular space above. Scale bar in microns.

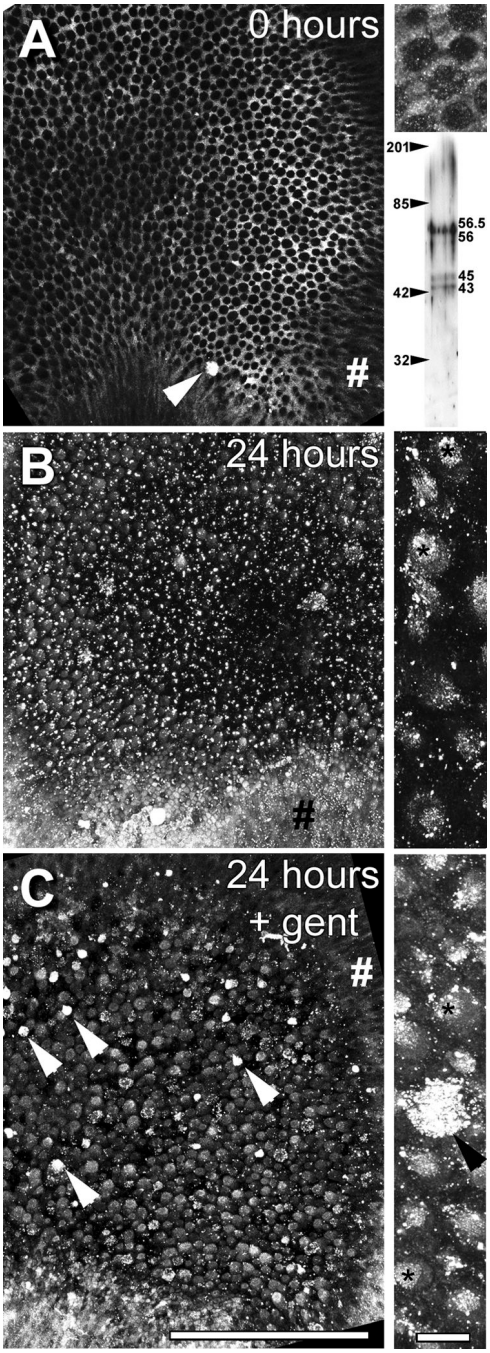

Figure 8.

(A) Bullfrog saccule (from right ear) fixed immediately after otolithic membrane removal and immunolabeled for cytokeratins. At low resolution, labeling is distinctly localized in supporting cell apices, outlining the round apices of hair cells. Note the intensely labeled extrusion near the growth zone (arrowhead). Upper inset on the right shows higher resolution projection image (of several focal planes) from the same saccule, with the labeling preferentially localized in the polygonal apices of supporting cells, and also as puncta in the round hair cell apex. Lower inset shows a Western blot of three distinct protein bands at 43, 45 and 56/56.5 kD for the cytokeratin antibody. Figures on the left indicate the position of the molecular weight markers. (B) Left saccule incubated in ACM only for 24 hours reveals loss of the distinctive cytokeratin

immunolabeling from supporting cell apices, and the appearance of bright puncta throughout the sensory epithelium, with generalized labeling of cells in the sensory epithelium. Inset on the right: Higher resolution projection image reveals preferential cytokeratin immunolabeling of round hair cell apices over adjacent supporting cells, with intense punctate labeling associated with the hair bundle (*), and elsewhere. (C) Right saccular explant treated with gentamicin for 6 hours and allowed to recover in ACM for 18 hours, reveals significant cytokeratin immunolabeling in the round hair cell apices. Note several intensely-labeled cells, probably extrusions (arrowheads). Inset on the right: Higher resolution projection reveals intense labeling in an extrusion and in many hair cell apices and bundles (*). Note the labeling of the transitional epithelium (#) in all low resolution images. Scale bars = 200 μm in main images and 10 μm in insets.

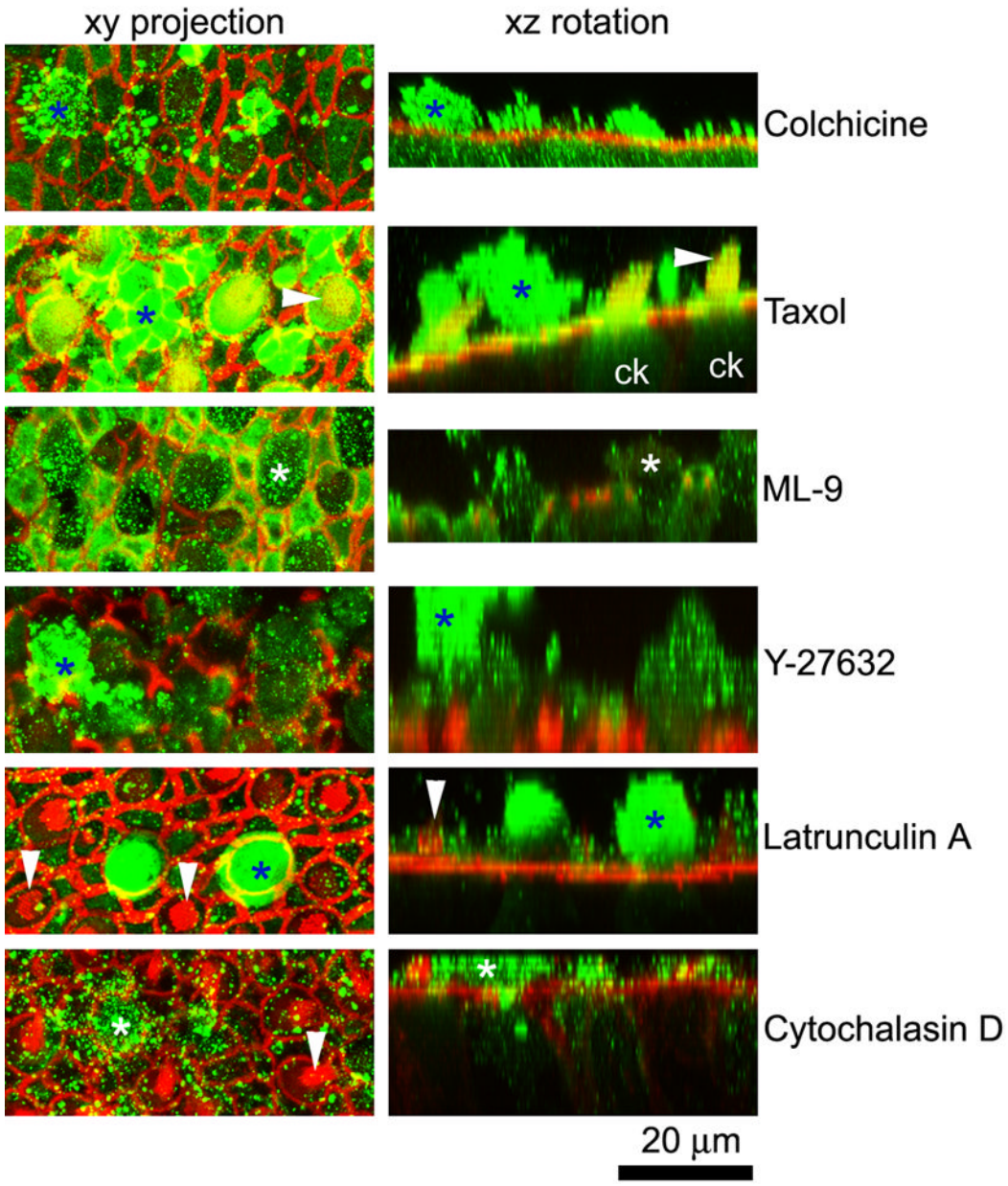

Figure 9.

Cytokeratin-labeled hair cell extrusions (*) are present in all explants, though far less frequently in latrunculin A and cytochalasin D-treated explants after gentamicin treatment. Phalloidin labeling for F-actin (red) indicates the borders of supporting cells and hair cells, some with their stereociliary bundles (arrowheads). The left column shows a projection of the optical planes incorporating the extrusion. The right column shows a 3-D rotation of the stack shown in the left column, indicating the extrusion (*). Note the cytokeratin labeling in hair cells (ck) in the taxol xz rotation panel. Numerous fluorescent speckles (green) also occurred above the sensory epithelium.

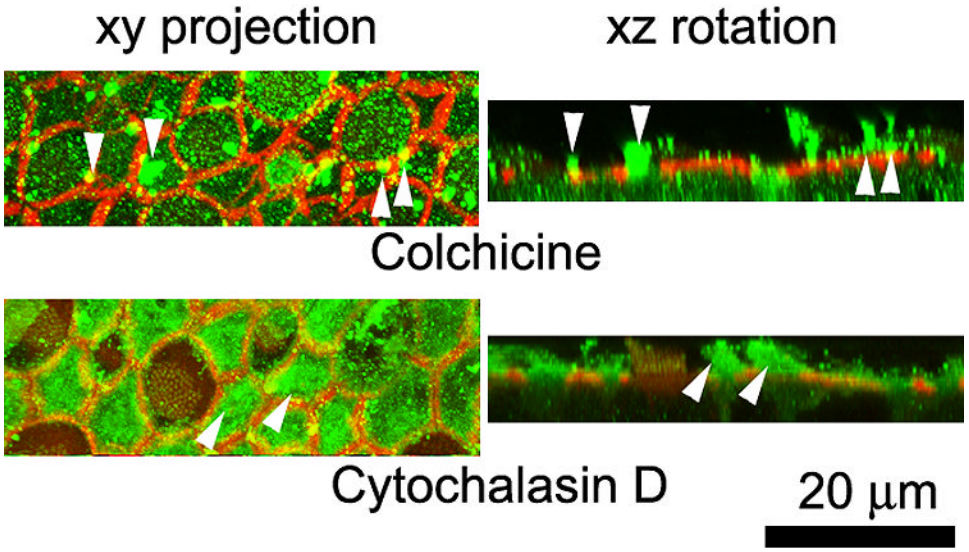

Figure 10.

Cytokeratin labeling (green) of supporting cell protrusions (arrowheads) in colchicine and cytochalasin-treated explants after gentamicin treatment. Phalloidin labeling for F-actin (red) indicates the borders of supporting cells and hair cells, some with their stereociliary bundles. The left column shows a projection of the optical planes incorporating the protrusion (arrowheads). The right column shows a 3-D rotation of the stack shown in the left column, indicating the protrusion (arrowheads).

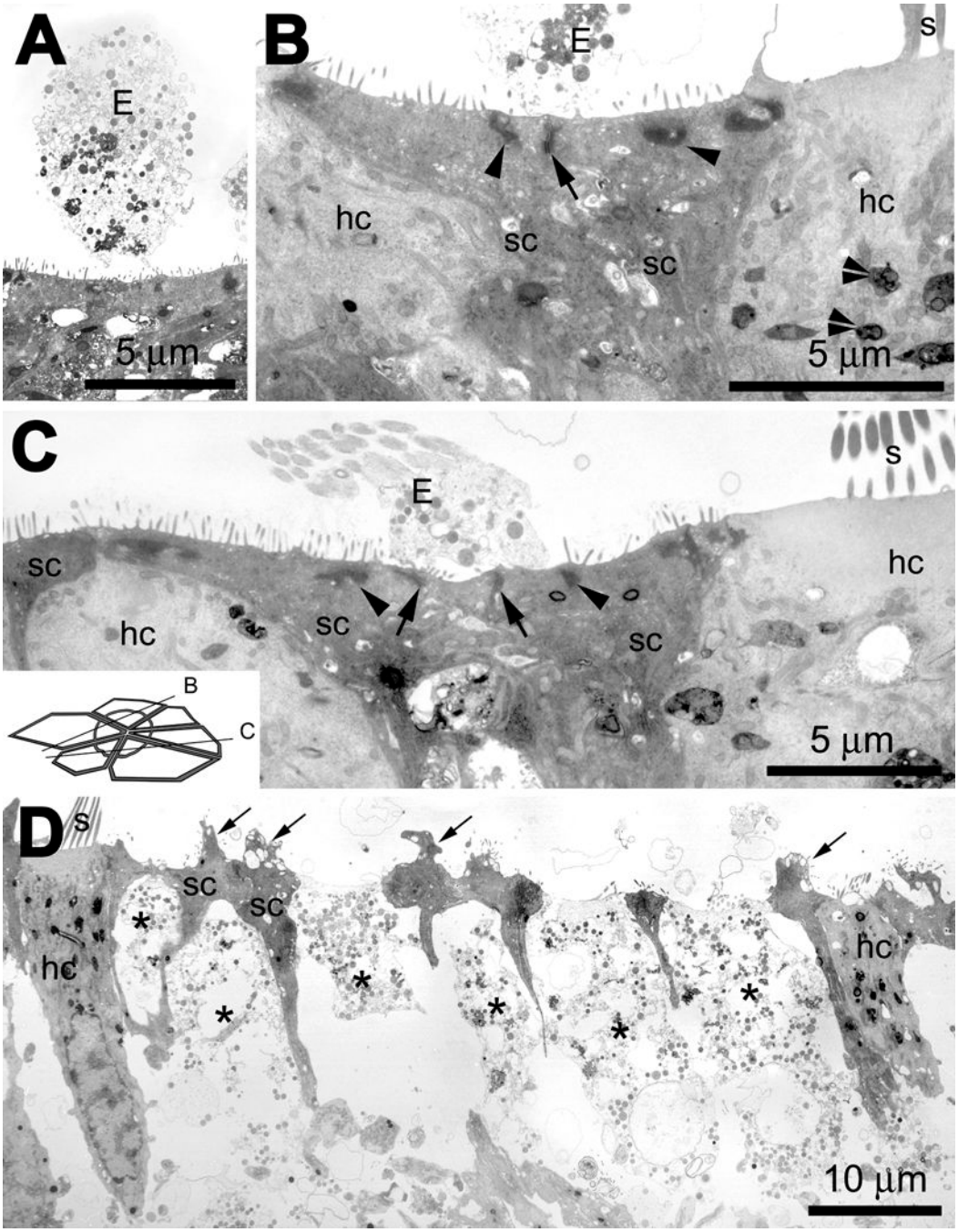

Figure 11.

(A) A low resolution image of an extrusion (E) with cytoplasmic contents above the sensory epithelium of an explant treated with gentamicin only. (B) In a gentamicin only-treated explant, extruded cellular material (E) is located above a sectioned scar formation; the expanded apices of two supporting cells (sc) meet and form a junctional complex (including tight junctions; arrow), with islands of electron-dense microfilamentous material (arrowheads) near the luminal membrane. Surviving hair cells (hc) contain electron-dense multi-vesiculated "gentamicin" bodies (double arrowheads). (C) Another example of a cross-sectioned supporting cell scar formation, where the expanded apices of three supporting cells (sc) forming two junctional complexes (including tight junctions, arrows) beneath extruded cellular material

(E). There are also islands of electron-dense, microfilamentous material (arrowheads) near the luminal membrane of these supporting cells. Inset shows approximate cross-sectional planes for panels B and C. (D). In gentamicin and cytochalasin D-treated explants, hair cells (hc) that survived drug administration are similar in density to hair cells in gentamicin-treated explants, with well-defined stereocilia protruding from the cuticular plate. Remnants of dead hair cells are emplaced within the sensory epithelium and highly electron-translucent (*), with little cytoplasmic material beneath the fragmenting cell apex. The supporting cell apices retained their junctional complexes, and often had cytoplasmic and vacuolated protrusions into the extracellular space (arrows).

Table 1

Concentration of specific cytoskeletal inhibitors and their actions.

Compound	Inhibitor of:	Concentration	Reference
Latrunculin A	*Actin polymerization*	5 μM	(Rosenblatt et al., 2001)
Cytochalasin D	*Actin polymerization*	1 μM	(Rosenblatt et al., 2001)
Taxol (Paclitaxel)	*Microtubule depolymerization*	0.1 μM	(Kim et al., 2002; Platts et al., 1999)
Colchicine	*Microtubule polymerization*	10 μM	(Platts et al., 1999)
ML-9	*Myosin light chain kinase*	200 μM	(Rosenblatt et al., 2001)
Y-27632	*Rho-kinase (blocks contraction)*	100 μM	(Rosenblatt et al., 2001)

Table 2

Hair bundle density (per 10,000 μm², +/− s.d.) after 24 hours explantation with various treatments.

Hair bundle Density (per 10,000 μm², +/− s.d.)							
	Left			Right			
	density	+/−	t-test vs left ACM	density	+/−	t-test vs *CL* explant[Φ]	t-test vs right *GT*-only explant[†]
in situ (n=3)	89.4	4.3	**	87.8	2.2	*n.s.*	-
24 hour explantation	Left saccule (control)[Φ]			Right saccule plus gentamicin			
ACM (4)	81.4	4.4	-	73.6[†]	3.6	***	-
Incubation with cytoskeletal disruption agents							
+ colchicine (3)	63.5	3.5	**	56.6	3.0	*	***
+ taxol (3)	80.4	6.6	*n.s.*	64.4	10.9	*	*n.s.*
+ ML-9 (4)	44.4	19.6	*	31.4	22.7	*	**
+ Y-27632 (2)[ǂ]	62.2	11.9	*	47.9	9.9	*	***
+ cytochalasin D (3)	76.5	4.6	*n.s.*	67.1	6.7	*	*n.s.*
+ latrunculin A (3)	84.0	3.1	*n.s.*	76.7	1.5	*	*n.s.*

n.s. not statistically significantly different

* $p < 0.05$

** $p < 0.01$

*** $p < 0.01$

CL contra-lateral

GT gentamicin

ǂ Note, only 2 morphologically intact explants treated with Y-27632 used for statistical analysis and imaging.